DIPOLE POLARIZATION EFFECTS ON HIGHLY-CHARGED-ION-ATOM ELECTRON CAPTURE

C. C. HAVENER, S. L. HOUGH, AND R. REJOUB

Physics Division, Oak Ridge National Laboratory,
Oak Ridge, Tennessee 37831-6372, USA

D. W. SAVIN AND M. SCHNELL

Columbia Astrophysics Laboratory, Columbia University,
New York, New York 10027-6601, USA

Dipole polarization effects are one of the dominant features in electron capture (EC) at low collision energies. The Oak Ridge National Laboratory ion-atom merged-beams apparatus has been used to explore low energy ion-atom EC for fundamental systems in the energy range of meV/u to keV/u. While the EC cross section often increases toward lower energies due to trajectory effects caused by the ion-induced dipole potential, several systems have been found where the cross section "oscillates" towards lower energies due to the quantal nature of the collisions. The merged-beams apparatus has recently been upgraded to take advantage of the high energy ion beams from the new Multicharged Ion Research Facility High Voltage Platform.

1. Polarization Effects in Low Energy Electron Capture

The electron capture (EC) process,

$$X^{q+} + A \rightarrow X^{(q-1)+} + A^{+} \tag{1}$$

by multicharged ions (X^{q+}) from neutral atoms (A) at low collision energies (meV/u - keV/u) is characterized by large cross sections, on the order of 10^{-14} - 10^{-16} cm^2 and is therefore important in many plasmas where ions and neutrals exist. Low energy EC is important for interpreting spectroscopic diagnostics and modeling of core, edge, and diverter regions of magnetically confined fusion plasmas. In astrophysics, electron capture by multicharged ions from H is important in planetary nebulae and H II regions. While scaling laws have been successful [1] in describing electron capture at higher energies, at low energies (< 1 keV/u), models must correctly handle both the quasi-molecular and fully quantum nature of the collision dynamics. Molecular Orbital Close Coupling (MOCC) calculations are deemed most appropriate but are difficult to perform and often have not been extended to eV/u energies and below.

A dominant feature in EC at eV/u energies is the effect that the ion-induced dipole has on the collision dynamics. During the collision process, as the ion and the neutral approach, a dipole is induced in the neutral atom, causing an attractive force between them. The resultant interaction potential is given by

$$V(r) = -\alpha \, {q^2}/{2r^4} \tag{2}$$

where α is the polarizability of the neutral, q is the charge of the ion , and r is the inter-nuclear separation. For eV/u collision energies and below, the attraction is strong enough to significantly modify the trajectories of the reactants and thereby affect the total capture cross section. Collisions with D rather than H experience the same attractive force but due to the larger mass have different trajectory effects and hence isotope effects can be present in the EC cross sections [2,3,4]. Indeed, the simple classical orbiting model (Gioumousis and Stevenson [5]), which uses a straightforward geometrical interpretation of orbits that decay into a reaction sphere influenced by the interaction potential of Eq. 2, predicts a strong *1/v* increase in the cross section at these low energies. This has been experimentally observed [6] for numerous ion-He and ion-molecule reactions where the cross sections typically converge to the Langevin cross section.

A theoretical survey [3] of EC for multicharged ions on H an D was performed using Landau-Zener cross section estimates and predicts that isotope effects and hence trajectory effects increase for higher incident charge and can occur at energies as high as a keV/u, especially for heavy highly charged ions. The Oak Ridge National Laboratory (ORNL) ion-atom merged-beams apparatus [7] provides benchmark fundamental measurements with H and D to explore trajectory effects.

2. Experimental Method

Low energy electron capture is performed at the Multicharged Ion Research Facility (MIRF) at ORNL using the ion-atom merged-beams apparatus which has previously been described in detail [7]. The newly upgraded version of the apparatus is shown in Figure 1. In this technique, intense relatively fast (keV) ion and atomic beams are merged producing center-of-mass collision energies from meV/u to keV/u. A neutral ground state hydrogen (or deuterium) beam is obtained by photodetachment of an H^- beam as it crosses the optical cavity of a

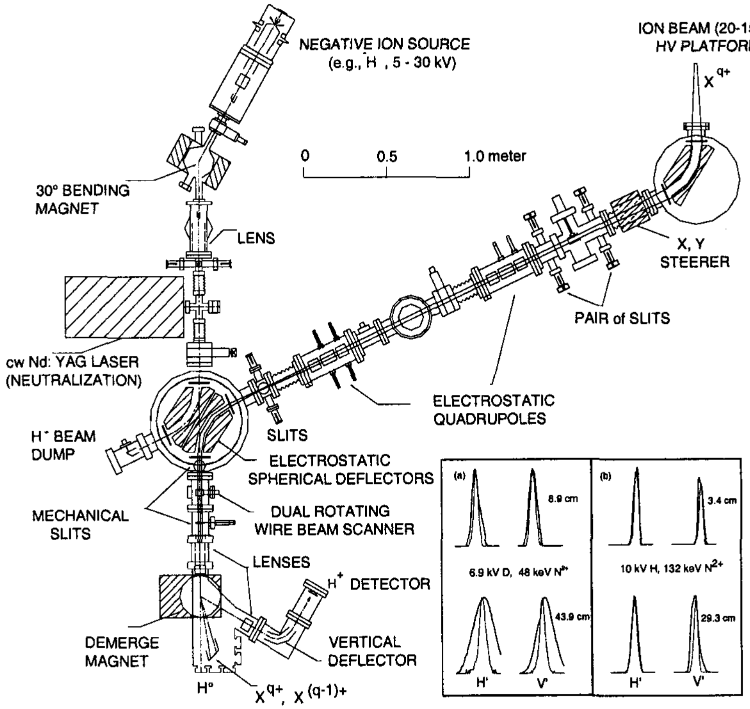

Figure 1. Schematic of the current ORNL ion-atom merged-beams apparatus. The inset compares +45 deg. (H') and -45 deg. (V') beam profiles at two positions along the merge path for the neutral (dashed) and the ion beam (solid) beams from the old CAPRICE ECR (a) and the new high velocity beams (b) from the HV platform.

1.06 μm cw Nd:YAG laser where kilowatts of continuous power circulate. The H^- is extracted from a duoplasmatron ion source. The ion and neutral beams interact along a field free region, after which H^+ product ions are magnetically separated from the primary beams. The neutral beam is monitored by measuring secondary electron emission from a stainless steel plate, and the intensity of the ion beam is measured by a Faraday cup. The product signal of H^+ ions is detected with a channel electron multiplier operated in pulse counting mode. The beam-beam signal rate (Hz) is extracted from (kHz) background with a two-beam modulation technique. The technique has been highly successful in providing benchmark EC total cross sections [8] for a variety of multiply charged ions in collisions with H and D.

The independently absolute charge transfer cross section is determined at each velocity from directly measurable parameters from the following formula,

$$\sigma = \frac{S\gamma q e^2 v_1 v_2}{I_1 I_2 v_r L < F >} \qquad (3)$$

where S is the signal count rate, q is the charge number of the ion, e is the electronic charge, I_1 and I_2 are the currents of the beams, v_1 and v_2 are the velocities of the beams, v_r is the relative velocity of the beams, L is the merge-path length, γ is the secondary electron emission coefficient of the neutral detector, and $<F>$ is the average form factor measuring the overlap of the beams. The form factor is estimated from two-dimensional measurements of the beam-beam overlap at three different positions along the merged path. The secondary electron emission coefficient γ is measured *in situ*. The velocities are calculated from the accelerating voltages of the beams, which include the estimated plasma potential shifts of the two sources (see, e.g., Ref [4]). The small (non-zero) angle between the merged beams must be determined along with the angular spreads of the interacting beams. It is the angular spread of the beams which effectively determine the energy spread of the measurements in the meV/u energy range.

The apparatus, shown schematically in Figure 1, has recently been upgraded and moved to accept beams from a CEA/Grenoble all-permanent magnet ECR ion source mounted on a 20-250 kV High Voltage (HV) platform. Upgrades to the apparatus include a dual rotating wire scanner which provides a real time indication of the divergence of the beams and a shorter merge path (47.1 to 32.5 cm) which increases the angular acceptance from 2.3 to 3.3 deg. in the lab frame. This increase transforms to a significant increase of angular collection in the center-of-mass frame where the products often exhibit significant angular scattering. A high transmission beam line from the HV platform contains two electrostatic quadrupole lenses and three sets of slits which are used to shape the beam and form a waste at the focal point of electrostatic spherical sector analyzers used to merge the ion and neutral beams. The inset in Figure 1 shows the improvements in the beam profiles compared to previous profiles with the (5-20 kV) ORNL CAPRICE ECR ion source. There is almost a factor of four decrease in the angular divergence of the ion beam. This translates into a significant improvement in the collision energy uncertainty and will allow access to lower energies with higher resolution. The higher velocity ion beam will make possible measurements with both H and D at energies below an eV/u. Previously, the higher velocity ion beams needed to match typical H beam velocities were not available from the CAPRICE ECR. Measurements at low center-of-mass collision energies had to be performed with D, especially for heavier lower charge ions.

3. Low Energy Electron Capture Measurements

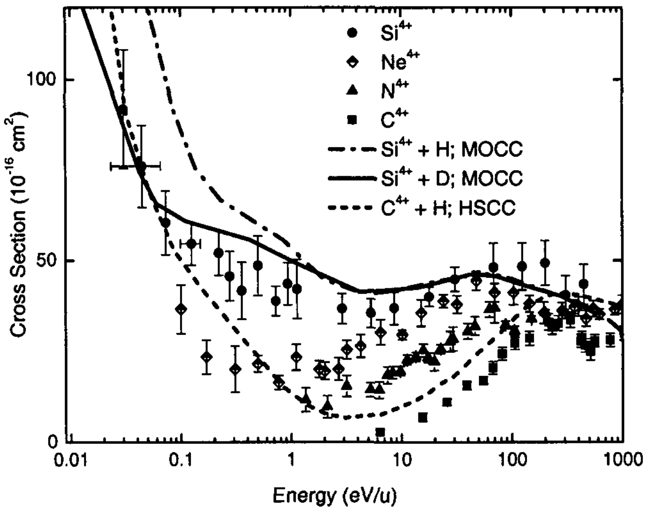

Figure 2. ORNL ion-atom merged-beams measurements for various q=4+ ions on H (D). For Si^{4+} and C^{4+} the measurements are compared to MOCC and HSCC calculations. See text for details.

ORNL merged-beam measurements for Si^{4+} [4], Ne^{4+} [9], N^{4+} [10] and C^{4+} [11] + H (or D) are shown in Figure 2 along with two MOCC calculations which extend to low energies for Si^{4+} [4]. Calculations for C^{4+} [12] from a more recently developed Hyperspherical Close Coupling (HSCC) method is also shown. All measurements below 10 eV/u were performed with D. As can be seen in the figure, all the q=4+ cross sections are similar around 1000 eV/u and scale with the empirical scaling law proposed by Phaneuf [1]. As the EC cross section decreases to lower energies the measurements show a marked difference for the different ions with different electron cores, over a factor of ten at 10 eV/u between C^{4+} and Si^{4+}. The measurements for Si^{4+} and Ne^{4+} have been extended low enough to observe the enhancement in the cross section due to trajectory effects caused by the ion-induced dipole potential. The Si^{4+} measurements show excellent agreement with the MOCC calculations for D; the MOCC calculations for H exhibit a large isotope effect indicative of trajectory effects. For C^{4+} the HSCC calculation also shows the $1/v$ increase. In fact all the other calculations (not shown) for the various $q=4+$ ions, benchmarked to the merged-beams measurements and extended to lower energies, exhibit a $1/v$ increase. The temporary decrease in the cross section or "oscillation" is due to the quantal nature of the electron capture process.

Of course, all ion-atom EC do not exhibit a Langevin increase at low energies. Systems whose capture channels are endoergic (e.g., Ne^{2+} + H [13]) or degenerate (e.g., He^{2+} + H [14]) decrease toward a lower energy threshold. According to Equation 2, however, one would expect that for exoergic collisions with ions of higher q, the trajectory effects would be greater and would move to higher energies [2,3]. ORNL merged-beams measurements for Cl^{7+} + D [15], the highest incident charge to date, show a surprisingly decreasing cross section. This sharp decrease can be understood when compared to MOCC calculations for N^{7+} + H (and D) where the large energy diabatic avoided crossings between initial and final potential curves leads to sharp decreases in the cross section. However, as indicated by the MOCC calculation for N^{7+}, the sharp decrease is eventually followed by a Langevin type increase for energies < 1 eV/u.

A collision system which is not predicted to follow this trend is N^{2+} + H and is shown in Figure 3. MOCC calculations by Bienstock *et al.* [16], Herrero *et al.* [17] and Barragan *et al.* [18] all show a cross section decreasing at lower energies. ORNL merged-beam measurements by Pieksma *et al.* [19] did not extend to low enough energies to establish the low energy dependence and have received new attention. This system is different from the $q=4+$ ions presented above because capture occurs to a state which involves excitation of the ion core. New measurements for this system are presented here with D using the old CAPRICE ECR and with H using the new HV platform. The measurements with D clearly show an increasing cross section toward lower energies in sharp contrast to the calculations. The measurements with H, which are now being performed with ion beams from the HV platform, are yet to be extended to low enough energies to test whether an isotope effect is present. Landau-Zener calculations (see Figure 3) have been performed which take into account the ion-induced dipole effects. These calculations show a Langevin type increase below 10 eV/u with a strong observable isotope effect below 0.1 eV/u.

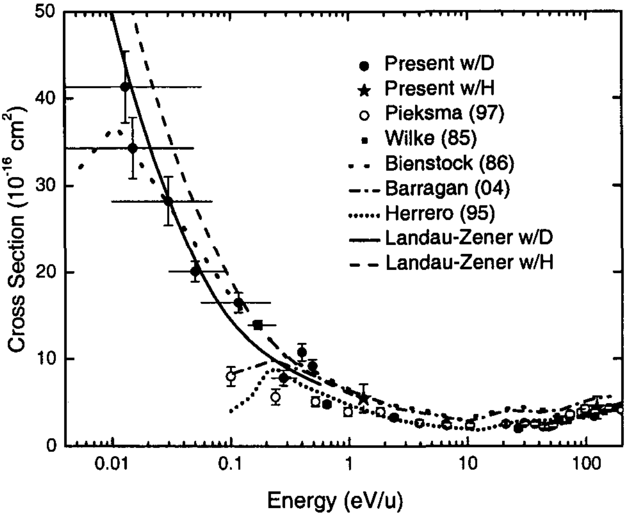

Figure 3. Present merged-beams measurements for N^{2+} with H and D are compared with our previous merged-beams measurements of Pieksma *et al.* [7] and with measurements of Wilke *et al.* [17]. Comparison is also made with a Landau-Zener and several MOCC calculations. See text.

4. Future Directions

The HV platform provides quality high velocity ion beams which allow much higher resolution measurements with both H and D below an eV/u. It should be possible to explore low energy EC for structure, e.g., due to Regge oscillations [21] or shape resonances [22]. The ion beams are now of sufficient intensity that state-selective EC may now be possible using photon spectroscopy. A Cs negative-ion sputter source can be exchanged with the duoplasmatron and used to provide a variety of multlielectron neutral beams, e.g., Li, B, Na, Al, P, K, Cr, Fe and molecular beams like O_2 and CH_2. The HV platform will soon be configured with a cold molecular ion source which will allow measurements with molecular ions.

Acknowledgments

This work is supported by the Division of Chemical Sciences, Office of Basic Energy Sciences and the Division of Applied Plasma Physics, Office of Fusion Energy Sciences, U.S. DoE, Contract No. DE-AC05-00OR22725 with UT-Battelle, LLC, and by the NASA SARA program under Work Order No. 10,060. DWS is supported in part by NASA SARA Grant NAG5-5420 and MS was supported in part by NSF Galactic Astronomy Program Award 0307203. SLH was appointed to the Higher Education Research Experiences at ORNL, administered by the Oak Ridge Institute for Science and Education.

References

1. R. A. Phaneuf, *Phys. Rev. A* **28**, 1310 (1983).
2. C. C. Havener, F. W. Meyer, and R. A. Phaneuf, in *Proceedings of the International Conference on the Physics of Electronic and Atomic Collisions, Brisbane* (IOP, Bristol, 1992), p. 381.
3. P. C. Stancil and B. Zygelman, *Phys. Rev. Lett.* **75**, 1495 (1995).
4. M. Pieksma, M. Gargaud, R. McCarroll, and C. C. Havener, *Phys. Rev. A* **54**, R13 (1996).
5. G. Gioumousis and D. P. Stevenson, *J. Chem. Phys.* **29**, 294 (1958).
6. K Okuno *et al.*, AIP Conference Proceedings **360** (AIP, New York, 1995), p. 867.
7. C. C. Havener, in *Accelerator-Based Atomic Physics Techniques and Applications,* edited by S. M. Shafroth and J. C. Austin (AIP, New York, 1997), p. 117.
8. C. C. Havener, in *The Physics of Multiply and Highly Charged Ions,* Vol. 2, (Kluwer Academic Publishers, Dordrecht, The Netherlands, 2003), p. 193.
9. C. C. Havener *et al.*, *Phys. Rev. A* **71**, 034702 (2005).
10. L. Folkerts *et al.*, *Phys. Rev. A* **51**, 3685 (1995).
11. F. W. Bliek *et al.*, *Phys. Rev. A* **56**, 426 (1997).
12. C-N Liu, A-T Le, and C. D. Lin, *Phys Rev A* ***68***, 062702 (2003).
13. T. Mroczkowski *et al.*, *Phys. Rev. A* **68**, 032721 (2003).
14. C. C. Havener *et al.*, *Phys. Rev. A* **71**, 042707 (2005).
15. J. S. Thompson *et al.*, *Phys. Rev. A* **63**, 012717 (2000).
16. S. Bienstock, A. Dalgarno, and T. G. Heil, *Phys. Rev. A* **33**, 2078 (1986).
17. B. Herrero, I. L. Cooper, A. S. Dickenson, and D. R. Flower, *Phys Rev A* **28**, 711 (1995).
18. P. Barragan, L. F. Errea, L. Mendez, A. Macias, I. Rabadan, and A. Riera, *Phys. Rev. A* **70,** 022707 (2004).

19. M. Pieksma, M. E. Bannister, W. Wu, and C. C. Havener, *Phys. Rev. A* **55,** 3526 (1997).
20. F. G. Wilke *et al.*, *J. Phys. B* **18,** 479 (1985).
21. J. H. Macek *et al.*, *Phys. Rev. Lett.* **93**, 183293 (2004).
22. M. Rittby *et al., J. Phys. B* **17**, L677 (1984).